RESEARCH ON VIBRATIONS IN THE TECHNOLOGICAL HEAD DEPENDING ON THE FEED RATE

ANTON PANDA[1,2], MAREK PRISLUPCAK[1]

[1]Faculty of Manufacturing Technologies with a seat in Presov, Technical University of Kosice, Bayerova 1, 080 01 Presov, Slovak Republic

[2]Institute of Technology and Business in Ceske Budejovice, Faculty of Technology, Department of Mechanical Engineering, Okruzni 10, Ceske Budejovice, Czech Republic

DOI: 10.17973/MMSJ.2025_12_2025076

anton.panda@tuke.sk

Abstrakt: The technology of abrasive water jet is one of the methods of division and cutting materials with the lowest impact on the environment, since water is the cutting tool, in our case with the addition of an abrasive. The experiments were carried out on one kind of material - steel HARDOX 500 with a thickness of 10 mm. The impact of the change of the technological head's feed rate on the size of the vibration acceleration amplitude and its frequency were examined. A database was created from the measured vibration values on the technological head and from that database the data was evaluated in selected softwares (LabVIEW, SignalExpress and Microsoft Excel). The results indicate that feed rates of 40 and 100 mm/min generate increased vibration intensity and reduced process stability, whereas the most stable cutting conditions occur at 50 mm/min, with feed rates of 200 and 400 mm/min also providing acceptable vibration behavior.

KEYWORDS

Technological head, frequency, vibration, water flow, abrasive water jet

1 INTRODUCTION

Since the beginning of human existence, people have developed various tools and sought diverse energy sources to achieve a safer, more comfortable, and efficient life. Over time, increasingly complex objects have been produced and continuously refined. The effectiveness of production processes has advanced with the discovery of new tools, materials, and energy sources [Panda 2014 & 2020, Nahornyi 2022, Pandova 2020, Harnicarova 2019, Panda 2021 & 2022, Sukhodub 2018 & 2019].

The use of water jet technology dates back to the 1970s, when it was primarily applied for cutting plastics and wood. Rapid development began in the late 1990s, when water jets started to be used for cutting, machining, and shaping metallic and non-metallic materials, ceramics, and composites. Today, water jet technology forms part of multi-technological automated systems, often integrated with additional technologies, robotic operations, and the use of significant amounts of abrasives and various auxiliary materials [Straka 2018a,b, Flegner 2019 & 2020, Gombar 2014, Pollak 2020a, Matiskova 2021].

Water-jet cutting is generally categorized into two types: pure water jet (WJM) without abrasives and abrasive water jet (AWJ), in which abrasive particles are added to the water jet. Water-jet material removal can be characterized as a high-velocity micro-erosion process. Its principle lies in the removal of material from the surface through the mechanical impact of a high-speed water jet with substantial kinetic energy applied to a small area [Mrkvica 2012, Monkova 2013, Michalik 2014]. This action causes the detachment of microscopic particles from the workpiece surface [Krenicky 2022]. To enhance the mechanical effect, abrasive particles are introduced into the jet.

The fundamental difference between WJM and AWJ lies in the cutting head design. The pure water jet head ends with a nozzle, whereas in the abrasive water jet, the high-pressure water enters a mixing chamber where it combines with abrasive particles. Another key distinction is the diameter of the outgoing jet. In WJM, the diameter depends on the nozzle size and typically ranges from 0.1 to 0.8 mm. In AWJ technology, the jet diameter is determined by the inner diameter of the focusing tube, commonly ranging from 1.2 to 2.5 mm.

When AWJ technology is used for machining and shaping materials, the process is influenced by several technological factors that induce vibrations [Saga 2019, Olejarova 2021]. These include the cutting head design, cutting speed, operating pressure, abrasive type, mass flow rate, and the jet's incidence angle.

2 TECHNOLOGICAL FACTORS ACTING (OPERATING) ON THE TECHNOLOGICAL HEAD

The key component of the entire system is the cutting head equipped with a nozzle, as it influences both the quality of the cut and the quality of the jet itself. For easier, faster, and more efficient tool handling, the cutting head is equipped with a bayonet cap. The advantage of bayonet caps lies in their self-centering mechanism, which eliminates the need for nozzle calibration when the head is changed. The activation and deactivation of the jet are controlled by a pneumatic on/off valve.

Feed rate represents the relative movement speed between the jet and the material being cut. During cutting, stagnation of the water flow can occur, causing a loss of energy and a deviation of the jet from its axis as it penetrates the material. By adjusting the feed rate, the following parameters can be influenced:

- depth of cut
- width and geometry of the kerf
- surface quality

Feed rate plays a crucial role in the overall effectiveness of the cutting process. Increasing the water pressure increases the jet velocity, resulting in greater available energy and enabling the cutting of thicker materials.

Pressure is one of the most important parameters affecting material separation. In AWJ technology, pressure is generated by a device known as a multiplier. After pressurization, the liquid flows through an accumulator, which reduces pressure pulsations due to fluid compression, and then through a transport system composed of thick-walled tubing into the cutting head. Inside the head, the fluid passes through a nozzle where the high-pressure water jet is formed. Fluid pressure influences jet expansion, which accelerates wear of the mixing tube, alters the mixing distance between abrasive and water, and reduces cutting efficiency. Higher working pressures increase abrasive particle fragmentation, which in turn affects the effectiveness and efficiency of the material-removal process.

Abrasives represent a critical component of AWJ technology. Abrasives consist of small particles mixed with the fluid, significantly enhancing the mechanical effect that enables the cutting of harder materials [Pollak 2020b]. The selection of abrasive material depends on economic, technical, and environmental considerations. Key factors affecting the cutting process include:

- Price – abrasive cost can represent up to 50% of total operating expenses.
- Density – higher density improves particle dynamics after leaving the cutting head.
- Hardness – influences the wear of the mixing tube and cutting speed; greater abrasive hardness increases cutting efficiency.
- Particle size and shape – characterized by roundness and circularity [Gulyaev 2022]. Particles with low circularity and high roundness are preferred. Particle size is expressed in MESH units (e.g., 60 mesh per inch), determined by sieving through standardized screens.
- Mass flow rate – increasing abrasive feed increases cutting depth and jet kinetic energy. Beyond a critical flow rate, cutting depth decreases and clogging of the mixing tube may occur. Higher mass flow typically reduces surface roughness, though most significant effects occur at greater depths.
- Ecological impact – abrasives should be environmentally safe and non-harmful to workers.
- Recyclability – reuse of abrasive material increases economic and environmental efficiency.

Incidence angle of the jet also affects the cutting process. The most common angle is 90°, which provides the most effective jet alignment perpendicular to the material surface. Changing the incidence angle alters both the quality and depth of the cut, as the jet's kinetic energy is distributed between vertical and horizontal components, modifying the material-erosion mechanism.

3 EXPERIMENTAL PART

3.1 Conditions of the experiment

The conditions for conducting the experiment were divided into three main categories: constant material parameters, constant technological parameters, and variable technological parameters.

Constant material parameters:

- Steel HARDOX 500, thickness 10 mm.

Constant technological parameters:

- Abrasive: Australian garnet
- Granularity: MESH 80
- Mass flow rate: 200 g/min
- Pressure: 280 MPa
- Diameter of the focusing tube: 1.02 mm
- Length of the focusing tube: 76 mm

Variable technological parameter:

- Feed rate: 40, 50, 100, 200, 400 mm/min.

3.2 Production system

The experimental work was carried out using the Multiplier PTV 1960 system (Fig. 1), operating at a maximum working pressure of 415 MPa and a maximum flow rate of 1.9 liters per minute. These parameters ensured stable high-pressure conditions and provided a suitable environment for the precise evaluation of vibration and technological effects during the cutting of HARDOX 500. The system was equipped with a PASER III TM technological head (Fig. 2) and a WJ1020–1Z–EKO CNC X–Y worktable (Fig. 3).

3.3 Measurement and data-processing

The measurement and data-processing system consisted of a piezoelectric IEPE uniaxial accelerometer Brüel & Kjær, model 4507-B-004 (TEDS-enabled) with a sensitivity of 100 mV/g. The accelerometer output was connected to an analog-to-digital converter NI USB-9233 by National Instruments, which provided high-resolution digital sampling of the vibration signals.

Data acquisition, signal conditioning, and subsequent processing were carried out using the LABVIEW SignalExpress environment (Fig. 4). This platform enabled real-time monitoring, recording, and analysis of vibration data throughout the experimental procedure.

Figure 1. Multiepier PTV 1960 system

Figure 2: Technological head PASER III TM

Figure 3. CNC X–Y worktable WJ1020–1Z–EKO

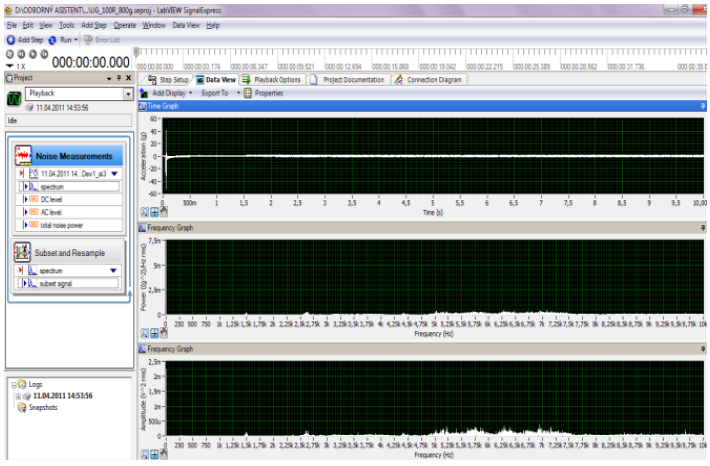

Figure 4. Work window in Labview SignalExpress

4 RESULTS AND DISCUSSION

4.1 Feed rate 40 mm/min

Figures 5 and 6 illustrate the vibration response of the technological head at a feed rate of 40 mm/min. The graphical relationship between the vibration acceleration amplitude and its corresponding envelope shows a single dominant high-frequency band. At this feed rate, however, the identified band exhibits the widest frequency range among all previously analyzed envelopes, extending from 5100 Hz to 7300 Hz. The maximum vibration acceleration reaches 0.004619 g at a frequency of 7000 Hz.

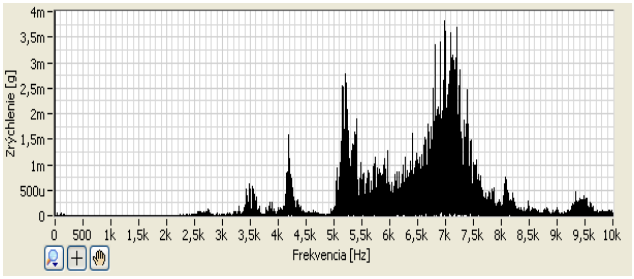

Figure 5. Graphical dependency of vibration acceleration amplitude and frequency – 40 mm/min

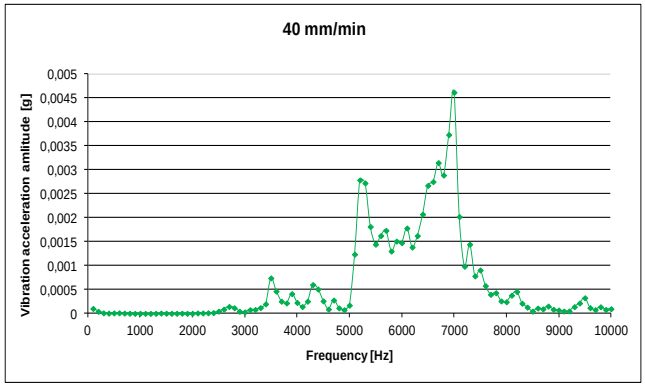

Figure 6. Frequency spectrum cover using the feed speed of 40 mm/min

4.2 Feed rate 50 mm/min

Based on the graphical dependence of vibration acceleration amplitudes shown in Figures 7 and 8, at a feed speed of 50 mm/min, the technological head begins to oscillate, producing distinct vibration effects. These are visible in the frequency spectrum as four elevated zones.

The first elevated zone occurs between 1500 Hz and 1700 Hz, with a maximum vibration acceleration of 0.000152 g at 1600 Hz. The second zone appears between 2600 Hz and 2900 Hz, where the maximum acceleration reaches 0.000337 g at 2700 Hz. The third zone extends from 3100 Hz to 3500 Hz, with a peak acceleration of 0.000468 g at 3300 Hz. The fourth and final elevated zone is observed between 5100 Hz and 5700 Hz, where the maximum vibration acceleration is 0.000303 g at 5400 Hz.

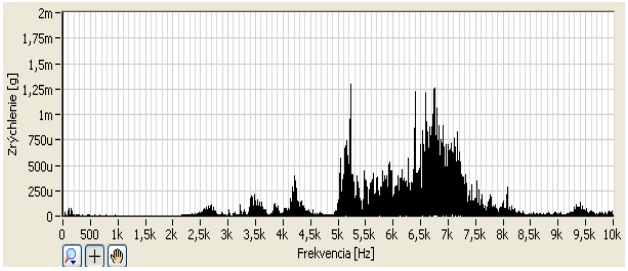

Figure 7. Graphical dependency of vibration acceleration amplitude and frequency – 50 mm/min

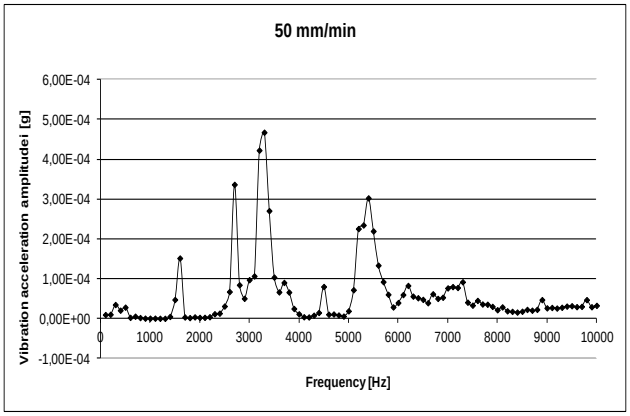

Figure 8. Frequency spectrum cover using the feed speed of 50 mm/min

4.3 Feed rate 100 mm/min

The effect of vibrations on the technological head at a feed speed of 100 mm/min is shown in Figures 9 and 10. The graphical dependence of the vibration acceleration amplitude and its corresponding envelope reveals a single elevated frequency band, ranging from 6800 Hz to 7300 Hz. The maximum vibration acceleration reaches 0.00453 g at a frequency of 7100 Hz.

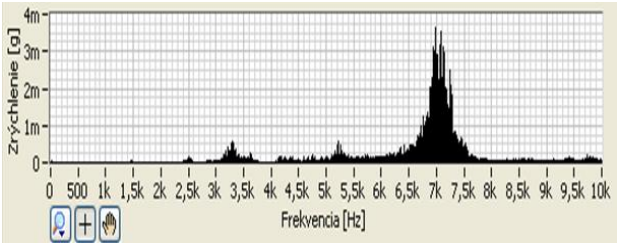

Figure 9. Graphical dependency of vibration acceleration amplitude and frequency – 100 mm/min

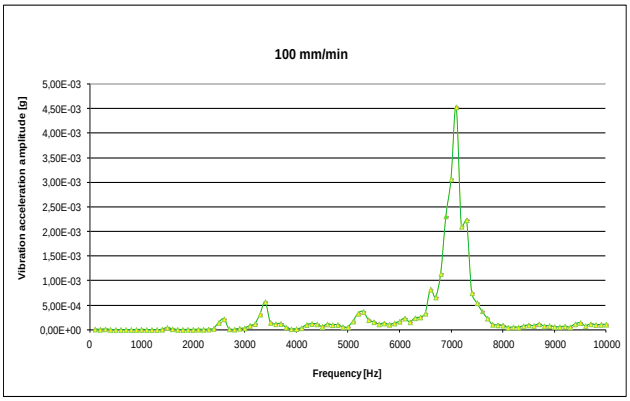

Figure 10. Frequency spectrum cover using the feed speed of 100 mm/min

4.4 Feed rate 200 mm/min

In Figures 11 and 12, we can observe the effects of vibrations on the technological head at an advance rate of 200 mm/min. The graphical dependency of the vibration acceleration amplitude and its corresponding envelope indicates three elevated frequency ranges. The first elevated band appears in the range from 3300 Hz to 3600 Hz, and the highest recorded acceleration value is 0.000431 g at a frequency of 3400 Hz.

The second elevated band occurs in the frequency range from 5200 Hz to 5500 Hz, where the maximum acceleration value reaches 0.000313 g at a frequency of 5300 Hz. The third and most prominent elevated frequency spectrum is found in the range from 7000 Hz to 7400 Hz, and the maximum vibration acceleration reaches 0.001086 g at a frequency of 7200 Hz.

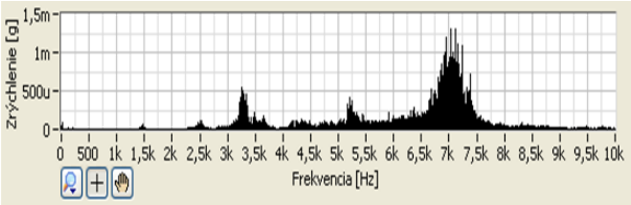

Figure 11. Graphical dependency of vibration acceleration amplitude and frequency – 200 mm/min

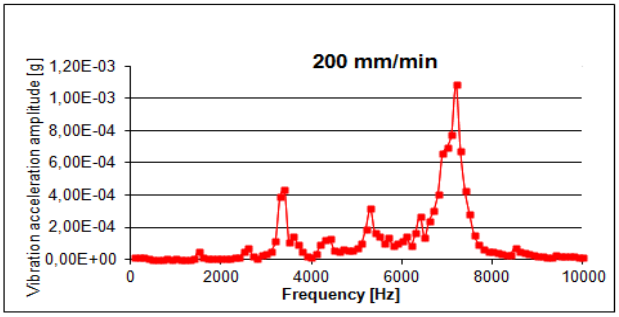

Figure 12. Frequency spectrum cover using the feed speed of 200 mm/min

4.5 Feed rate 400 mm/min

The effect of the strength of vibrations on the technological head when cutting the HARDOX 500 material at an advance rate of 400 mm/min is depicted in Figures 13 and 14. The graphical dependency of the vibration acceleration amplitude and frequency, together with its corresponding envelope, indicates an increase in vibration amplitude in two distinct frequency bands. The first elevated band occurs within the frequency range of 3300 Hz to 3700 Hz, where the maximum acceleration value reaches 0.000423 g at a frequency of 3300 Hz. The second band exhibits even more pronounced elevated values, ranging from 7100 Hz to 7500 Hz, with a maximum vibration acceleration amplitude of 0.001677 g at a frequency of 7200 Hz.

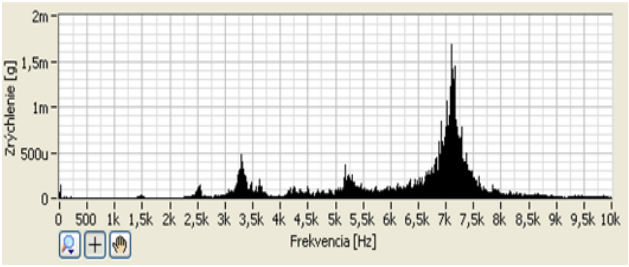

Figure 13. Graphical dependency of vibration acceleration amplitude and frequency – 400 mm/min

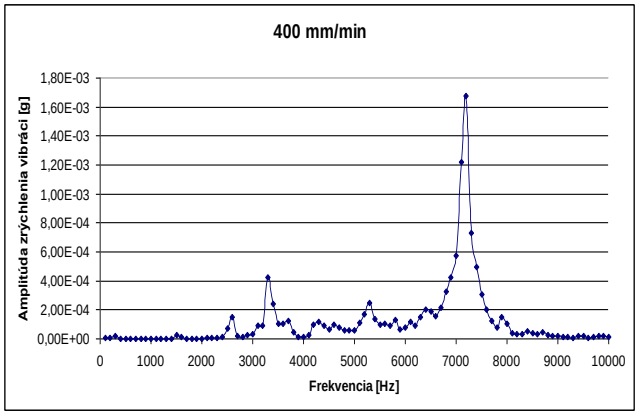

Figure 14. Frequency spectrum cover using the feed speed of 400 mm/min

5 CONCLUSIONS

The results of the assessment indicate that, within the tested range, a feed rate of 50 mm/min is the most suitable for machining HARDOX 500 steel. At this feed speed, the vibration acceleration amplitude reached its lowest values, making it the most stable and efficient option in the analyzed conditions. Favourable vibration characteristics were also observed at feed rates of 200 mm/min and 400 mm/min. At 200 mm/min, the maximum vibration acceleration amplitude was 0.001086 g at 7200 Hz, while at 400 mm/min the maximum amplitude reached 0.001677 g at the same frequency. Significantly higher and less desirable vibration values were recorded at feed rates of 40 mm/min and 100 mm/min. A feed rate of 40 mm/min is not recommended for machining HARDOX 500, as it resulted in the broadest and highest frequency band (5100–7300 Hz) with a maximum vibration acceleration amplitude of 0.004619 g at 7000 Hz. Similarly, a feed rate of 100 mm/min is also not advisable, since despite slightly lower vibration values compared to 40 mm/min, it still produced an increased frequency range (6700–7300 Hz) and a maximum amplitude of 0.003065 g at 7100 Hz.

Overall, the findings suggest that lower stability and higher vibration intensities occur at 40 and 100 mm/min, while the most stable operation is achieved at 50 mm/min, with acceptable performance also at 200 and 400 mm/min.

ACKNOWLEDGMENTS

This work was supported by the project KEGA: 008TUKE-4/2025 of Scientific Grant Agency of the Ministry of education, science, research and sport of the Slovak Republic and the Slovak Academy of Sciences.

REFERENCES

[Flegner 2019] Flegner, P., Kacur, J., Durdan, M., Laciak, M. Processing a measured vibroacoustic signal for rock type recognition in rotary drilling technology. Measurement, Journal of the International Measurement Confederation, 2019, Vol. 134, pp. 451-467.

[Flegner 2020] Flegner, P., Kacur, J., Durdan, M., Laciak, M. Statistical Process Control Charts Applied to Rock Disintegration Quality Improvement. Applied Sciences, 2020, Vol. 10, No. 23, pp. 1-26.

[Gombar 2014] Gombar, M., Vagaska, A., Koraus, A., Rackova, P. Application of Structural Equation Modelling to Cybersecurity Risk Analysis in the Era of Industry 4.0. Mathematics, 2024, Vol. 12, pp. 2-28.

[Gulyaev 2022] Gulyaev, P., et al. Particle and Particle Agglomerate Size Monitoring by Scanning Probe Microscope. Applied Sciences, 2022, Vol. 12, No. 4. DOI: 10.3390/app12042183.

[Harnicarova 2019] Harnicarova, M., et al. Study of the influence of the structural grain size on the mechanical properties of technical materials, Materialwissenschaft und Werkstofftechnik, 2019, Vol. 50, pp. 635-645. ISSN 0933-5137.

[Krenicky 2022] Krenicky, T., Olejarova, S., Servatka, M. Assessment of the Influence of Selected Technological Parameters on the Morphology Parameters of the Cutting Surfaces of the Hardox 500 Material Cut by Abrasive Water Jet Technology. Materials, 2022, Vol. 15, 1381. https://doi.org/10.3390/ma15041381.

[Matiskova 2021] Matiskova, D., Cakurda, T., Marasova, D., Balara, A. Determination of the Function of the Course of the Static Property of PAMs as Actuators in Industrial Robotics. Applied sciences, 2021, Vol. 11, No. 16, pp. 1-16, ISSN 2076-3417.

[Michalik 2014] Zajac, J., Hatala, M., Mital, D. and Fecova, V. Monitoring surface roughness of thin-walled components from steel C45 machining down and up milling. Measurement, 2014, Vol. 58, pp. 416-428. ISSN 0263-2241.

[Monkova 2013] Monkova, K., Monka, P., Jakubeczyova, D. The research of the high speed steels produced by powder and casting metallurgy from the view of tool cutting life. Applied Mechanics and Materials, 2013, Vol. 302, pp. 269-274.

[Mrkvica 2012] Mrkvica, I., Janos, M., Sysel, P. Cutting efficiency by drilling with tools from different materials. Advanced Materials Research, 2012, Vols. 538-541, pp. 1327-1331. ISSN1022-6680.

[Nahornyi 2022] Nahornyi, V., et al. Method of Using the Correlation between the Surface Roughness of Metallic Materials and the Sound Generated during the Controlled Machining Process. Materials, 2022, Vol. 15, 823. https://doi.org/10.3390/ma15030823.

[Olejarova 2021] Olejarova, S. and Krenicky, T. Water Jet Technology: Experimental Verification of the Input Factors Variation Influence on the Generated Vibration Levels and Frequency Spectra. Materials, 2021, Vol. 14, 4281.

[Panda 2014] Panda, A., Prislupcak, M., Pandova, I. Progressive Technology Diagnostics and Factors Affecting Machinability. Applied Mechanics and Materials, 2014, Vol. 616, pp. 183-190. ISSN 1660-9336.

[Panda 2020] Panda, A., et al. A novel method for online monitoring of surface quality and predicting tool wear conditions in machining of materials. International Journal of Advanced Manufacturing Technology, 2020, Vol. 123, No. 9-10, pp. 3599-3612. ISSN 0268-3768.

[Panda 2021] Panda, A., et al. Increasing of wear resistance of linear block-polyurethanes by thermal processing methods. MM Science Journal, 2021, Vol. October, pp. 4731-4735.

[Panda 2022] Panda, A., et al. Ecotoxicity Study of New Composite Materials Based on Epoxy Matrix DER-331 Filled with Biocides Used for Industrial Applications. Polymers, 2022, Vol. 14, No. 16, 3275. ISSN 2073-4360.

[Pandova 2020] Pandova, I., et al. A study of using natural sorbent to reduce iron cations from aqueous solutions. International Journal of Environmental Research and Public Health, 2020, Vol. 17, No. 10, 3686.

[Pollak 2020a] Polllak, M., Torokova, M., Kocisko, M. Utilization of generative design tools in designing components necessary for 3D printing done by a robot. TEM Journal, 2020, Vol. 9, No. 3, pp. 868-872. ISSN 2217-8309.

[Pollak 2020b] Polllak, M., Kocisko, M., Paulisin, D., Baron, P. Measurement of unidirectional pose accuracy and repeatability of the collaborative robot UR5. Advances in Mechanical Engineering, 2020, Vol. 12, No. 12, pp. 1-21.

[Saga 2019] Saga, M., Vasko, M., Handrik, M., Kopas, P. Contribution to random vibration numerical simulation and optimisation of nonlinear mechanical systems. Scientific Journal of Silesian University of Technology - series Transport, 2019, Vol. 103, pp. 143-154. DOI: 10.20858/sjsutst. 2019.103.11.

[Straka 2018a] Straka, L., Hasova, S. Optimization of material removal rate and tool wear rate of Cu electrode in die-sinking EDM of tool steel. International Journal of Advanced Manufacturing Technology, 2018, Vol. 97, pp. 2647-2654.

[Straka 2018b] Straka, L., Hasova, S. Prediction of the heat-affected zone of tool steel EN X37CrMoV5-1 after die-sinking electrical discharge machining. Journal of Engineering Manufacture, 2018, Vol. 232, No. 8, pp. 1395-1406.

[Sukhodub 2018] Sukhodub, L, Panda, A, Dyadyura,K, Pandova, I, Krenicky, T. The design criteria for biodegradable magnesium alloy implants. MM Science Journal, 2018, Vol. December, pp. 2673-2679.

[Sukhodub 2019] Sukhodub, L., Panda, A., Sukhodub, L., Kumeda, M., Baron, P. Hydroxyapatite and zinc oxide based two-layer coating, deposited on Ti6Al4V substrate. MM Science Journal, 2019, Vol December, pp. 3494-3499.

CONTACT:
Prof. Eng. Anton Panda, PhD.
Faculty of Manufacturing Technologies with a seat in Presov
Technical University of Kosice
Sturova 31, 080 001 Presov, Slovak Republic
e-mail: anton.panda@tuke.sk